Shape optimization of a Roots blower rotor profile using CFD model with a coupled Adjoint-Sculpting method

Neeraj BIKRAMADITYA[1]*, Sham RANE[2], Ahmed KOVACEVIC[3]

[1]City, University of London, UK
Neeraj.Bikramaditya@city.ac.uk

* Corresponding Author

ABSTRACT

A Roots Blower operates as a rotary positive displacement machine. Minimizing clearance gaps between the rotors and housing is crucial for enhancing volumetric efficiency. One of the options is optimizing the configurations of the leakage gap over the rotor tip. Utilizing prediction tools for this purpose is preferable to manual numerical simulations. Moreover, shape optimization tools are instrumental in identifying optimal design solutions. In this study, the combination of Fluent-Adjoint solver and RBF-morph technology, known as Adjoint-Sculpting, is employed to explore design conceptualization. Adjoint-Sculpting leverages Fluent-Adjoint's predictive capabilities to estimate the effects of shape changes based on observable targets, complemented by RBF fluid morphing to accommodate these changes without necessitating fluid volume remeshing. Notably, RBF morphing maintains the quality of the base volume mesh. To investigate optimization methods for positive displacement machines, a 2D simplified Roots blower is considered, with the Adjoint methodology compared against conventional CFD results. Subsequently, variations in observables and different rotor tip shapes and combinations are examined using RBF fluid morphing. The findings from this study demonstrate that utilizing Fluent-Adjoint and RBF morph enables more effective and efficient prediction of tip shapes compared to conventional methods. Additionally, the study highlights the limitations of shape optimization using moving wall boundary conditions. These insights hold significance for compressor technology, facilitating the implementation of rotor tip design changes and streamlining resource-intensive conventional CFD calculations.

1. INTRODUCTION

Positive displacement compressors exhibit variations in design and operation based on their intended applications. Twin-screw compressors and Roots blowers are extensively utilized in commercial and industrial settings. In rotary positive displacement machines, rotating parts are enclosed inside a stationary component known as the casing. Principally, the compression in these machines occurs inside these enclosed chambers when the rotor rotates.
The Roots blower (Figure 1(a)) has a straight lobe, so whenever it rotates, it sucks in air and delivers it to the discharge without internal compression and Figure 1(b) provides a sectional view of the Roots blower assembly, indicating the terminology for clearances. When the lobe passes over the blower inlet, a finite volume of air is trapped and carried around the chamber by the lobes. The air is then discharged at the blower outlet. As the lobes continue to rotate, the pressure increases in the reservoir beyond the blower outlet. Consequently, the pressure difference between the discharge and suction causes air to flow back from the reservoir to the low-pressure regions through these clearances. To ensure the air flows without lubrication (or oil-free) and ensure reliable operations, it is crucial to maintain a gap between the rotating and stationary parts. The maximum leakage losses occur through the radial clearance gap between the casing and the rotor.

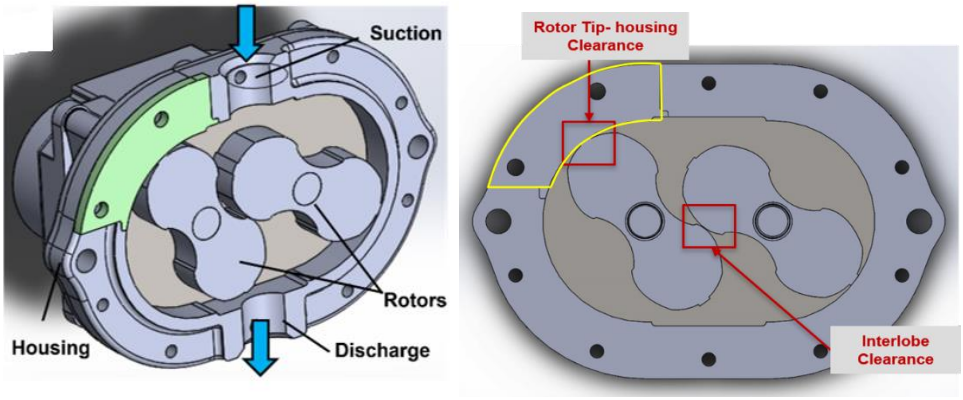

Despite the satisfactory efficiency of these compressors, there remains substantial potential for internal design improvements. Researchers have undertaken optimization efforts aimed at enhancing efficiency through simulations based on their practical experiences. Historically, these optimizations were often conducted through trial and error, involving experimental adjustments to parameters such as casing design, rotor profiles, inlet/outlet configurations, and injection ports and others. Both experimental and numerically-based approaches rely on experiential knowledge of flow patterns and physical parameters, introducing uncertainty. To address this uncertainty and facilitate rapid design iterations, researchers have leveraged commercially available tools for predictive analysis. The Fluent Adjoint solver is among the primary tools utilized for this purpose. However, it is worth noting that some of the changes predicted and implemented by the Adjoint solver may not always yield optimal results. Morphed shapes can degrade the quality of the volume mesh, presenting challenges. To mitigate these challenges, researchers across aeronautical, aerospace, automotive, medical device, and other domains have adopted special morphing techniques such as RBF. This method, based on Radial Basis Functions, preserves the quality of the volume mesh by exclusively modifying the surface mesh during morphing.
In shape design optimization, determining the most effective representation of the surface remains an ongoing concern. Contemporary research endeavours often employ B-splines, which offer flexibility in surface definition. By adjusting the polynomial degree and the number of control points, researchers can manipulate the number of design variables and surface fidelity. Consequently, design variables can be aligned with individual grid points on the surface by selecting a linear polynomial and an appropriate number of control points.

The initial industrial advancements in shape optimization within fluid mechanics contexts emerged primarily within aeronautical and aerospace engineering domains. One of the most renowned instances in this domain involves the optimization of airfoil designs, as documented in Carlton *et al*. (1964), wherein optimal profiles for minimizing drag-related issues were computed utilizing shape sensitivity analyses. The new concept by Kyle *et al*. (1999) introduced a continuous Adjoint formulation for aerodynamic design optimization on unstructured grids computing sensitivities of objective functions with respect to design variables. Biancolini *et al*. (2010) introduced an advanced application of Radial Basis Function (RBF) morphing technique in the context of coupled Computational Fluid Dynamics (CFD) and Computational Structural Mechanics (CSM) analysis for aeroelastic simulations. Biancolini *et al*. (2011) introduced the application of Radial Basis Functions (RBF) for mesh morphing and smoothing. In his work, he presented a practical example of mesh morphing using Fluent, a popular CFD software, and RBF Morph, a commercial software package specialized in RBF-based mesh morphing. The example demonstrates the application of RBF morphing techniques to deform a computational mesh while maintaining its quality and accuracy. Mathew *et al*. (2011) provided a comprehensive comparison of mesh morphing methods for 3D shape optimization, highlighting their strengths, weaknesses, and potential applications in engineering and scientific simulations. His research study contributed to the understanding of mesh morphing techniques and their role in optimizing complex geometries for various purposes. Lombardi *et al*. (2013) presented RBFs as a promising approach for addressing inter-grid interpolation and mesh motion challenges in FSI simulations, offering flexibility, accuracy, and versatility in handling complex fluid-structure interactions. Biancolini *et al*. (2017) identified potential research directions and areas for further development of fast RBF techniques in engineering applications. It suggested avenues for improving algorithmic efficiency, extending the capabilities of RBF methods to new domains, and integrating RBF-based approaches into existing engineering workflows. Papoutsis-Kiachagias *et al*. (2018) research paper underscored the importance of advanced optimization techniques such as the continuous Adjoint method and RBF morpher in achieving efficient and effective aerodynamic design for automotive applications.

Porziani *et al*. (2019) discussed the practical implications of mesh morphing-enabled shape sculpting for industrial design and engineering. It highlighted the potential for accelerating product development cycles, reducing design iterations, and enhancing overall product performance through automated shape optimization. Porziani *et al*. (2020), this study explains the principles of BGM, a bio-inspired optimization algorithm that mimics natural growth processes to evolve optimal shapes. BGM iteratively modifies the geometry of structural parts based on predefined objectives and constraints, leading to improved performance characteristics. Stefano *et al*. (2021) in his paper outlined the optimization framework used for automatic optimization driven by mesh morphing surface sculpting and BGM. It describes the iterative process of shape modification, simulation, and optimization, emphasizing the role of BGM in guiding the optimization process.

Industries and researchers across various sectors such as aerospace, automotive, medical devices, and others have actively pursued shape optimization endeavors and process enhancements by leveraging advancements in technology. Typically, they employ readily accessible software tools to generate new shapes through optimization techniques. Conversely, researchers in the field of compressor technology have shown limited interest in shape optimization using available predictive technologies. Therefore, there is a need to investigate and scrutinize the optimization outcomes, as well as identify issues pertinent to the application of these methods within the operational context of compressors. This study aims to assess the efficacy of shape optimization and morphing software following validation against Conventional CFD simulations. Additionally, to speed up the shape optimization process, study focusing on the exploration of Fluent-Sculpting methodologies is also carried out to check the feasibility of this technology.

2. Methodology

To execute shape optimization in this study, Fluent-Adjoint solver is mainly studied. For the morphing of the shape predicted by Adjoint solver, RBF-Morph software for fluids will be adopted. Fluent-Sculpting technology will also be studied for the utilization of the atomization of the process.

2.1 Fluent- Adjoint Solver for Shape Optimization

The Adjoint method is a specialized mathematical tool that expands the capabilities of a Computational Fluid Dynamics (CFD) solution by offering detailed sensitivity information regarding the performance of a fluid system under specific boundary conditions. The sensitivity data provided by an Adjoint solver fulfills a crucial requirement in gradient-based shape optimization, rendering it a distinctive and potent engineering tool for design enhancement. Additionally, Adjoint data can contribute to the refinement of solver numerical accuracy. Regions exhibiting high sensitivity indicate areas within the flow where discretization errors may exert a significant impact. This knowledge aids in guiding mesh refinement strategies to enhance the accuracy of the flow solution.

Once the Adjoint analysis is conducted, it serves as a guide for implementing intelligent design alterations to a system. The sensitivity data obtained from the Adjoint analysis offers insights into the effect of surface movement across the entire geometry. Design modifications are most impactful when applied to regions of high sensitivity, as even minor adjustments can yield substantial improvements in the engineering metrics of interest. This principle, known as making proportional changes to a system based on local sensitivity, forms the basis of the simple gradient algorithm utilized for design optimization.

2.1.1 Mathematical Background**:** The method begins with a flow solution, q, and the input vector to the problem, c. Here, the quantity of interest is J((q(c); c) function of q and the residual of the N-S equations R_i(q(c); c) = 0.

By defining Lagrangian, L, with the vector of Lagragian multipliers, $\tilde{q}^T$, which is known as Adjoint solution variables, the equation can be written as;

$$\frac{dJ}{dc} = \frac{dq}{dc}\left(\frac{\partial J}{\partial q} + \tilde{q}^T \frac{\partial R}{\partial q}\right) + \frac{\partial J}{\partial c} + \tilde{q}^T \frac{\partial R}{\partial c} \tag{1}$$

If Adjoint solution variable, $\tilde{q}^T$, chosen such that;

$$\frac{\partial J}{\partial q} + \tilde{q}^T \frac{\partial R}{\partial q} = O \; i.e. \; \left[\frac{\partial R}{\partial q}\right]^T \tilde{q} = -\left[\frac{\partial J}{\partial q}\right]^T \; ; where \; \tilde{q} \; is \; the \; solution$$

$$\frac{dJ}{dc} = \frac{\partial J}{\partial c} + \tilde{q}^T \frac{\partial R}{\partial c} \tag{2}$$

Equation (1) is simplified into a linear problem which is Equation (2), where LHS term of Equation (2) is Adjoint sensitivities.

2.1.2 Adjoint sensitivities: Principally, the sensitivity equation is evaluated at each node of the CFD mesh. In case of shape sensitivity, the input vector, c, is defined as the respective locations (x, y, z) in mesh. The LHS of Equation (2) is the total sensitivity of J with respect to (x, y, z) of nodes of mesh. RHS first term ($\frac{\partial J}{\partial c}$) is the change in the J due to the change in the positions (x, y, z) of nodes. RHS second term is the change in J due to the sensitivity of the flow solution with respect to the changes in the node location, and this depends on the Adjoint solution. These derivatives are calculated using the expressions derived from the definitions of the observables and Naviers-Stokes discretized equations.

2.2 Fluent- RBF Fluid Morph for Surface Morphing

Mesh morphing involves altering the shape of a computational grid by adjusting the positions of surface nodes exclusively. The proposed morphing technique relies on Radial Basis Function (RBF). Radial Basis Functions (RBF) are mathematical tools capable of interpolating a function at arbitrary points in space based on discrete point data. In the context of mesh morphing, RBFs are employed to smoothly modify the mesh geometry using a set of source points and their corresponding displacements.

When using RBFs for mesh morphing, the three components of a displacement field (in Equation (3)) are interpolated in space based on a cloud of control points, referred to here as RBF centres or source points. These interpolated displacements are then utilized to update the positions of the mesh nodes slated for morphing. In basic terms, Equation (3) is known as a generic interpolation function for multidimensional data.

$$s(x) = \sum_{i=1}^{N} \gamma_i \varphi\left(\left\|x - x_{k_i}\right\|\right) + h(x) \tag{3}$$

Where $s(x)$ is an interpolator, φ is a Radial Basic Function (scalar function of Euclidian distance between source and target points), γ_i is a weight of the radial basis function and *h(x)* is the polynomial that allows to retrieve the polynomial fraction of interpolation and rigid motions analytically The *h(x)* has order one less than the radial function, φ. *N* is the number of source points having positions as x_{k_i} in space x. The common RBFs are shown below in Table 1 for $r = \|x - x_k\|$;

Table 1. Radial Basis Functions

Type	**Equations**
Spline type	r^n, n is odd
Thin Plate Spline	$r^n \log(r)$, n is even
Multi-quadratic (MQ)	$\sqrt{1 + r^2}$
Inverse Multi-quadratic	$1/\sqrt{1 + r^2}$
Inverse Quadratic	$1/(1 + r^2)$
Gaussian	e^{-r^2}

Generally, RBF needs to be slightly modified to guarantee the existence and uniqueness of the solution, which can be obtained by adding polynomial part *h(x)* as given in Equation (3). The mesh morphing applications have to handle vector field of displacements. In these cases, each component is interpolated as an independent scalar field given in Equation (4). The βi (i=1,2,3,4) is the coefficients of linear polynomial.

$$s(j) = \sum_{i=1}^{N} r_i^j \varphi\left(j - j_{k_i}\right) + \beta_1^j + \beta_2^j x + B_3^j y + \beta_4^j z \;\; ; where\; j = (x, y, z) \tag{4}$$

The morphing action is restricted to the desired zones of the mesh simply prescribing a null motion to those nodes that wrap the affected area. The more detail about theory can be referred from RBF morph (2020).

3. Computational Domain & Setup

The computational domain utilized for the shape optimization investigation aligns with the framework outlined by Neeraj *et al*. (2024). In this study, the domain is simplified to a 2D representation (refer to Figure 1) employing the Multiple Reference Frame (MRF) approach. Adjoint calculations are conducted based on the initial Computational Fluid Dynamics (CFD) simulation, incorporating the conditions and parameters specified in Table 2. Notably, the base CFD model employed in this simulation operates under steady-state conditions, with the rotor tip serving as a wall boundary. The setup closely follows that of the study outlined in Neeraj *et al* (2024) with a thickness of 5mm which is in Z direction (into the paper in this case). The inlet and outlet boundary conditions are fixed pressure boundary conditions.

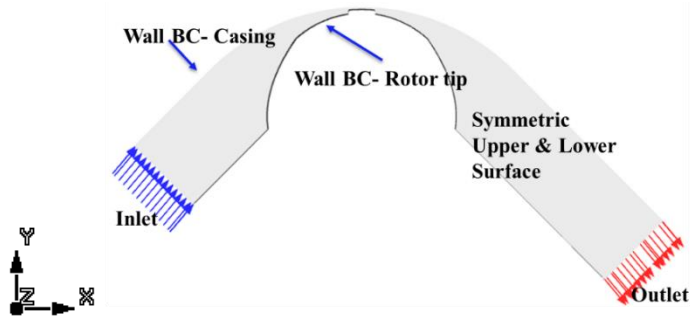

Figure 1: Base-Computational domain and Boundary Conditions

Table 2. Base CFD Solver Set-up.

Items	Specification	Items	Specification
Solver	Pressure based	**Spatial discretization**	2nd Order upwind
Turbulence	K-ω SST, K-ε, LES	**Turbulence numeric**	2nd Order upwind
Fluid Medium	Air	**Gradient**	Green-Gauss node
P-V Coupling	Coupled	**Flux-type**	Rhie-chow: mom based

Table 3. Adjoint Solver Set-up

Items	Specification	Items	Specification
Gradient	Green-Gauss Cell based	**Coupling**	Partial
Pressure	Standard	**Courant Number**	1
Momentum	First OD upwind	**URF-adjoint continuity & mom**	0.6
Energy	Adjoint Energy	**URF-adjoint flow rate & energy**	0.6

The solver settings and under-relaxation factors utilized for the Adjoint solution are outlined in Table 3. Upon completion of the Adjoint calculation, the software identifies regions exhibiting high shape sensitivities based on predefined optimization criteria. Determining the specific areas for morphing necessitates user input, typically involving considerations such as restriction on wall movement, as observed in the current study with the casing wall. Subsequently, when employing RBF fluid morphing, users have the flexibility to select one or more regions for modification, along with specifying the direction of movement. In this investigation, adjustments were permitted for the rotor tip surface and symmetry walls, while constraints were imposed on the remaining surfaces of the computational domain due to the casing wall boundary condition.

4. Results & Discussion

3.1 Fluent Adjoint and Conventional CFD result verification

For the verification of the accuracy of result predicted by Adjoint solution, the mass flow rate was compared with CFD simulation of manual shape modification as indicated by Adjoint. Both simulations used same base CFD model setup. The Mass flow rate was computed using surface integral of a plane located near exit of the tip (at X=0.0028m). The same plane is considered for defining the observable for Adjoint calculation. The objective was set to decrease the mass flow rate by 20% for Adjoint solver.

Table 4. Adjoint Solver Set-up with Surface movement allocation

Observable	Mass Flow Rate (ṁ) Kg/s	**Change allowed**	Rotor Tip surface and axial walls
Morph Method	Radial Basis Function	**Change restriction**	Casing wall
Smoothness	1		

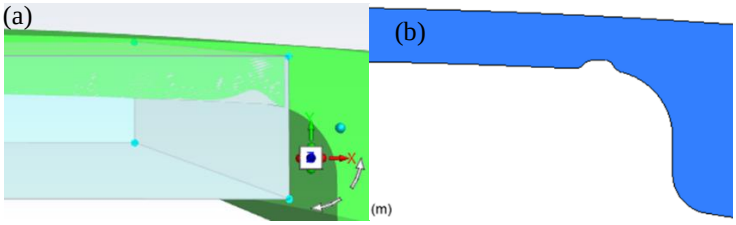

Figure 2: (a) Adjoint Predicted shape (Green) (b) CFD Manual shape change

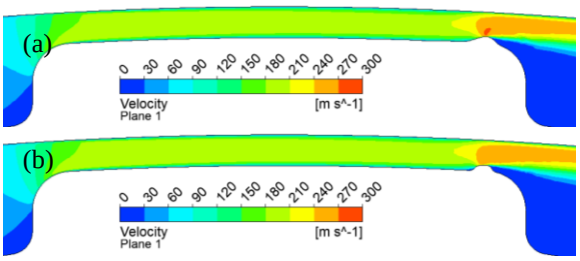

Figure 3: Velocity contour of (a) Adjoint (b) CFD

Table 5. Mass Flow Rate Comparison

Case	ṁ(g/min)	Δ(ṁ) (g/min)	Δ(ṁ)%
Base	47.61		
Adjoint	39.71	7.9	0.0131
CFD-Conventional	39.66	7.95	0.0132

Figure 2 is showing the domain after the shape optimization using (a) Adjoint solver and (b) CFD Conventional method. First, the shape prediction was obtained by Adjoint solver (Figure. 2(a)) and then conventional CFD modelling was done based to reflect change as closely as possible(Figure 2(b)). Although Conventional modelling has been tried to mimic the same design change but it is important to note that change accomodated will have some differences in shape and size. The velocity contour (Figure 3) comparison have shown some minor changes in velocity at the top of circular restriction where Adjoint solution indicates higher velocity than Conventional calculation. It is possible that mesh refinement changed after the Adjoint morphing took place. Mass Flow rate comparison is given in the Table 5. It shows that both solution have producing same leakage flow with minor differences. The discrepancy between both cases are mostly because of difference in the tip profile and mesh refinement level. This indicates the accuracy of Adjoint predictions. Based on this verification, shapes prediction by other observable and automation of process by Fluent -Scultping were analysed to obtain the new profile of tip.

3.2 Conventional Shape optimization using RBF Morph

The utilization of RBF morphing facilitates the combination of shapes, a process that typically requires significant time and numerous steps using conventional modelling methods. Drawing from the approach outlined by Neeraj et al. (2024), Conventional trials involving equal and unequal cavity shapes were conducted. RBF morphing was employed

to modify surfaces based on the initial cavity tip shapes. Various cases were explored with different restrictions and clearance gap openings, aiming for minimal effort in experimentation. Once a morphing solution was established for one case, subsequent cases were modelled by simply adjusting the gap heights (H1/H2/H3) in the input text file. In other words, these manual design modifications using modelling and meshing tools are time-consuming. The Figure 4 shows the schematic of the domain geometry setup, with H1 representing the clearance gap at the tip entrance, H2 denoting the cavity size, and H3 indicating the gap at the rotor exit. Table 6 provides a comparison of mass flow rates among different cases. Velocity contour results depicted in Figure 5 suggest that reducing the exit clearance leads to decreased leakage flow, thereby improving efficiency. When the cavity is of double depth than depth of tip entrance and exit, which is case6, the leakage occurs minimum as compared to all shapes. This clearly indicates that there is specific relation of depths between cavity and other part of tip which gives best results. This design indicated more improved leakage flow than the case with cavity of height (H2) of 1.4 mm ($\dot{m}$=0.000622 Kg/s) (Neeraj *et al* (2024), Figure 13(b)). The tip shape with more restriction at the exit of the tip (Case3) and optimum cavity height (Case6) yields reduction in leakage. The less deep cavity(H2) causes the flow to recirculate more strongly in the wall vicinity than deeper cavity thereby preventing back flows more efficiently. It is important to note that the case1 is the normal tip case which does not have the cavity.

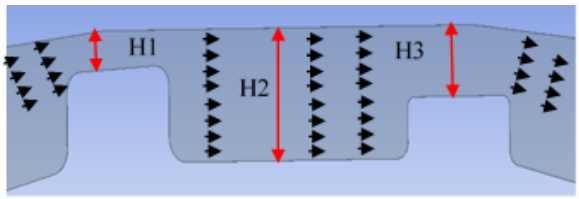

Figure 4: Model Schematic of Domain based on Tip shape configuration

Table 6. Mass Flow rate comparison

Case	Design(H1/H2/H3)	$\dot{m}$(g/min)	Δ%
Case1	0.4/0.4/0.4 (mm)	47.99	Base
Case2	1.2/0.4/1.2 (mm)	47.35	-1.3%
Case3	1.2/0.8/0.4 (mm)	39.57	-17.5%
Case4	0.4/0.8/1.2 (mm)	45.55	-5.1%
Case5	0.8/0.4/0.8 (mm)	47.84	-0.3%
Case6	0.4/0.8/0.4 (mm)	37.25	-22.4%

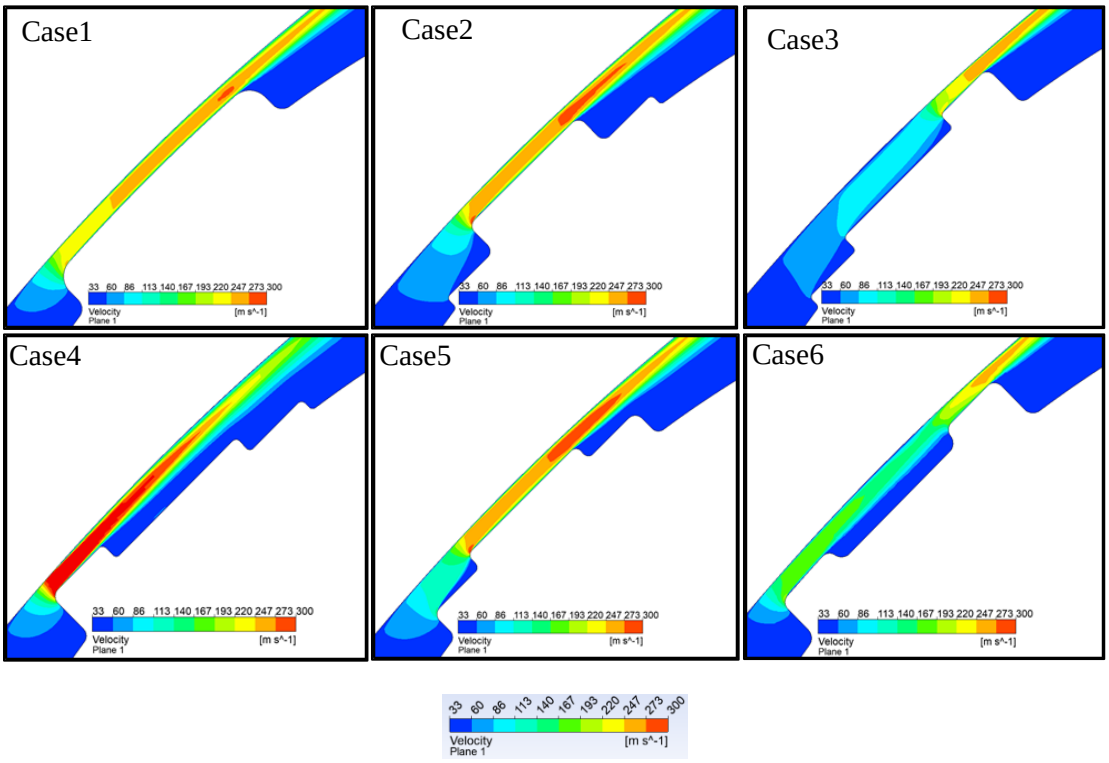

Figure 5: Velocity contour comparison at RPM2000 and PR1.6

3.3 Fluent Adjoint- Drag observable

The objective was set to increase "Drag" in tip-profile (of rotor tip) to reduce the leakage flow. The complete tip region (light blue box, a bounding box) was allowed for shape change including tip surface and, and Adjoint predicted a new surface based on the desired target of drag. The overlapping of new and old shape can be seen in the Figure 6 (a) with bumps representing the new shape.

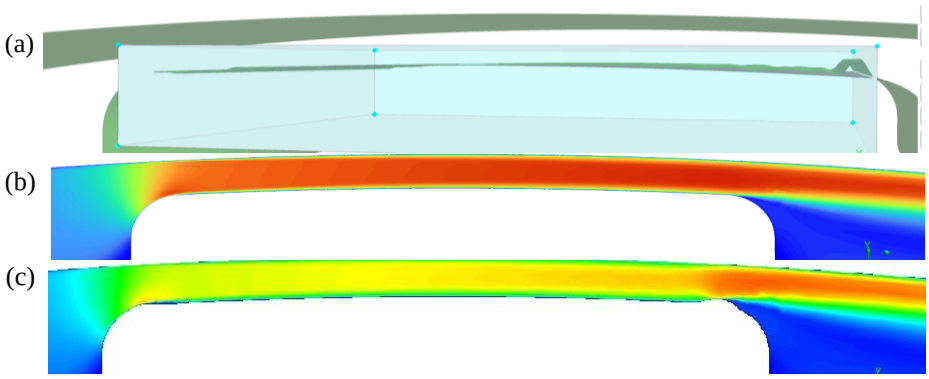

Figure 6: (a) Modified shape predicted by Adjoint Solver (b) & (c) Velocity contours of Base and Predicted model at RPM2000 and PR1.6 respectively

Also, the Adjoint predicts the shape change irrespective of its morphing results of volume mesh. In the first case for the target objective of 10% decrement, the volume meshing failed due to negative volumes. A second case with 0.5% of target which allowed smaller change in the tip surface resulted no negative volumes after morphing. The drag increment by 0.016 reduced the leakage flow by 15% (shown in Figure 7) with wavy surface of rotor and higher bump at the exit of the rotor. The flow velocity became slower in clearance gap. Figure 6(b) and (c) indicates the similar pattern as in the case Adjoint with mass flow rate and Conventional CFD simulation.

Table 7. Drag coefficient, mass flow rate and absolute maximum velocity comparison

Case	Drag Co-efficient	ṁ (g/min)	Vmag (max)
Base	8.699	47.94	273m/s
Adjoint- Prediction	8.711	40.62	265m/s

3.4 Fluent- Sculpting

Fluent-Sculpting involves coupling the Adjoint solution with surface morphing via RBF fluid morphing. After defining pressure as an observable and performing calculations with the Adjoint solver, the surface normal shape sensitivity is assessed. This assessment identifies the location with the highest sensitivity of the local observable variable, indicating where design improvements are needed. Using the location of highest shape sensitivity, RBF morph is applied for surface morphing with the "adj-filt" option in Fluent-Adjoint. This process, which couples Fluent-Adjoint and RBF Morph, is known as Sculpting. Furthermore, for extended improvement, several iterations on the same RBF solutions from the coupling can be performed without redefining the normal shape sensitivity. The shape modifications and velocity contours resulting from the Sculpting process, considering two iterations, are shown in Figures 7 and 8, respectively. Each iteration used for the improvement employed the same morphing topology to accommodate the changes in the tip surface.

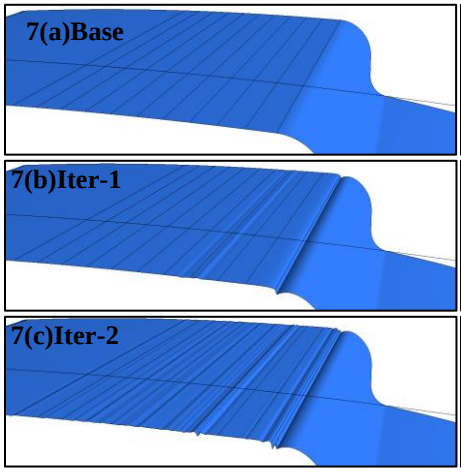

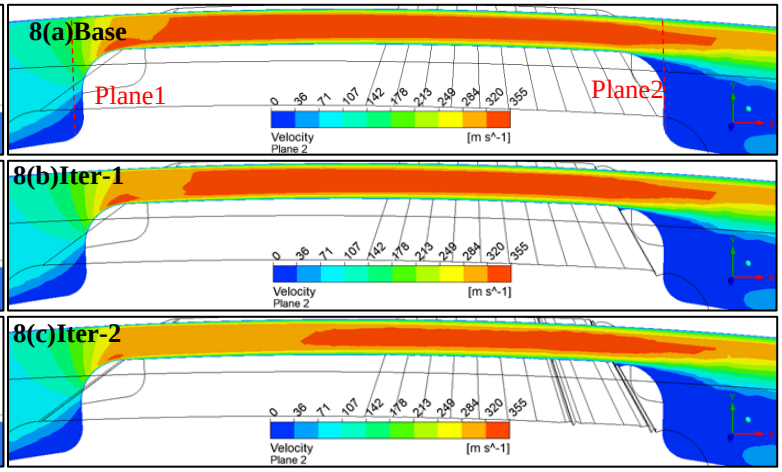

Figure 7: Morphed shapes after Sculpting **Figure 8:** Velocity contour comparison & Planes

Figures 7(a), (b) and (c) show the sequential change in the shape of tip surface near the exit of the rotor. Figure 8(a), (b) and (c) are the contours based on the changes done by morphing shown in Figure 7. The surfaces contain increased number of wavy profile as it continues to run for next iterations. These wavy surfaces have increased the pressure drop, and thereby decreased the leakage flow given in Table 8. Iter-1 shows slightly lower pressure drop than base case but Iter-2 has higher drop than base and Iter-1. The Plane 1 is Rotor-in Plane1 and Plane 2 is Rotor-exit Plan 2 are defined at entrance and exit of the rotor tip throughout the thickness of 5mm respectively.

Table 8. Pressure drop and mass flow rate comparison (Plane1 at x=-0.003m & Plane2 at x=0.003m)

Case	Rotor-in Plane1	Rotor-exit Plane2	ΔP(Plane1-Plane2)	ṁ(g/min) @ Plane2	%Δ(ṁ)
Base	152844 [Pa]	92512.2 [Pa]	60331.8 [Pa]	45	
Iter-1	152998 [Pa]	92601.6 [Pa]	60397.4 [Pa]	44.28	-2%
Iter-2	153492 [Pa]	92967.1 [Pa]	60524.9 [Pa]	42.6	-5%

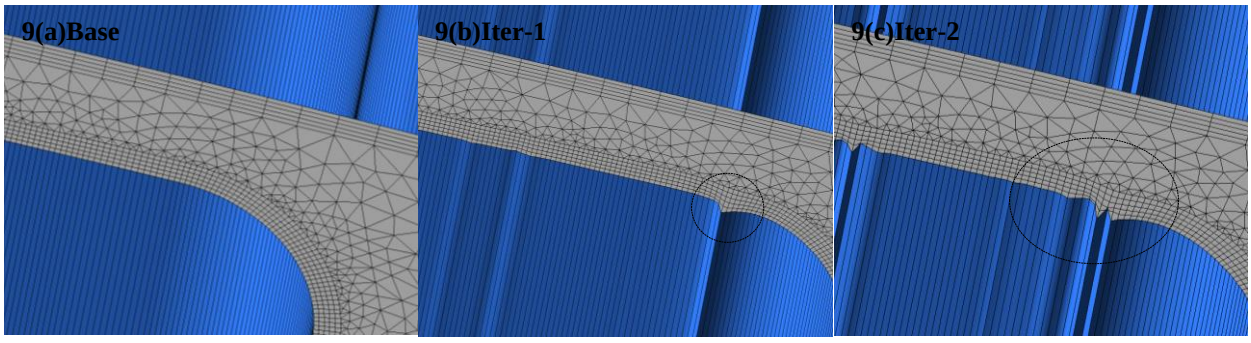

Figure 9: RBF Morph Mesh Quality comparison for Fluent-Sculpting

Figure 9 illustrates the mesh quality preserved by the solver through automated iterations using the Fluent-Sculpting method. These results indicate that morphing allocates the movement of nodes or cells in the vicinity of the modified location without affecting other nearby areas. In this case, only a few immediate boundary layers were adjusted within the fluid volume. The blue surface represents the rotor tip surface, while the grey areas (planes) depict the mesh, showing the fluid volume from the casing to the rotor tip.

This automated approach to shape optimization offers advantages compared to Adjoint morphing alone, as Adjoint morphing has demonstrated limitations regarding negative volume mesh post-morphing. RBF morphing addresses these issues by enabling designated surfaces to move in defined and in flexible ways, thereby mitigating fluid volume mesh-related errors.

4. CONCLUSIONS AND FUTURE WORK

Adjoint-based shape optimization was carried out for the tip profile of a 2D simplified Roots blower and validated through manual shape-change for conventional CFD flow simulations. Subsequently, other observables were explored to predict the tip's shape, yielding preliminary results showing a consistent pattern of restriction at the tip exit to reduce leakage flow. The findings regarding cavity shape in the tip profile suggested that cavities with optimal depths led to improved leakage flow. Determining the optimum depth involved adjusting the heights while disregarding deeper depths (H2), as deeper depths tended to allow more leakage.

Throughout this investigation, it was observed that while the base unsteady CFD simulation could be utilized for Adjoint simulation, the Adjoint solver exclusively performed steady simulations. Therefore, unsteady simulations could be employed after completing mesh morphing via the Adjoint solver. Additionally, it was noted that when using a bounding box to restrict zones or surfaces for morphing, it must encompass the integral plane or boundaries defined for the observable allocation.

In the subsequent phase of the study, Fluent-Sculpting was attempted to automate shape optimization. It was found that employing the RBF Fluid morph tool to impose restrictions and control movements on surfaces proved highly advantageous, as it preserved superior mesh quality compared to conventional morphing methods employed by the Adjoint solver.

In future, it will be crucial to apply these methods to 3D domains of Roots blowers and Screw compressors by preserving the vertex data from the morphed shape.

NOMENCLATURE

PR	Pressure Ratio	(-)	RHS	Right Hand Side	(-)
RPM	Rotation Per Minute	(-)	LHS	Left Hand Side	(-)
MRF	Moving Reference Frame	(-)	ITER	Iterations	(-)
CFD	Computational Fluid Dynamics	(-)	N	Number	(-)
RBF	Radial Basis Function	(-)			

Symbol

$\dot{m}$	Mass Flow Rate	(g/min)
Δ	Change or difference	(-)
βi	Coefficient of Polynomial	(-)
H	Height	(mm)

REFERENCES

ANSYS, Inc. https://www.ansys.com/en-gb/resource-center/webinar/ansys-fluent-adjoint-solver-based-optimization

Bikramaditya, N., Rane, S., Kovacevic, A., Patel, B. (2024): CFD Analysis of Leakage Flow in Radial Tip Gap of Roots Blower, 13th International Conference on Compressors and Their Systems. ICCS 2023. Springer Proceedings in Energy. Springer, Cham. https://doi.org/10.1007/978-3-031-42663-6_4

Biancolini, M.E. (2017): Fast Radial Basis Functions for Engineering Applications. Springer, Cham (2017). https://doi.org/10.1007/978-3-319-75011-8

Biancolini, M.E. & Cella, U (2010): An advanced RBF morph application: coupled CFD CSM aeroelastic analysis of a full aircraft model and comparison to experimental data. In: MIRA International Vehicle Aerodynamics Conference, Grove, pp. 243– 258 (2010)

Biancolini, M.E. (2011): Mesh morphing and smoothing by means of radial basis functions (RBF): a practical example using Fluent and RBF Morph. In: Handbook of Research on Computational Science and Engineering: Theory and Practice, pp. 347–380. IGI Global (2011)

H. W. Carlson and W. D. Middleton (1964): A numerical method for the design of camber surfaces of supersonic wings with arbitrary planforms, NASA Technical report, (1964)

Kiachagias, E. M. Papoutsis, S. Porziani, C, Groth, Biancolini, M. E., E, Costa & K. C, Giannakoglou (2018): Aerodynamic optimization of car shapes using the continuous adjoint method and an RBF morpher. Computational Methods in Applied Sciences, vol 48. Springer, Cham. https://doi.org/10.1007/978-3-319-89988-6_11

Lombardi, M., Parolini, N., Quarteroni, A (2013): Radial basis functions for inter-grid interpolation and mesh motion in FSI problems. Comput. Methods Appl. Mech. Eng. 256, 117

Matthew L. Staten, Steven J. Owe1, Suzanne M. Shontz, Andrew G. Salinger, and Todd S. Coffey (2011): A comparison of mesh morphing methods for 3D shape optimization. In: Proceedings of the 20th International Meshing Roundtable, pp. 293–311. Springer, Cham (2011).

Porziani, S., Groth, C., Waldman, W., Biancolini, M.E (2020): Automatic shape optimisation of structural parts driven by BGM and RBF mesh morphing. Int. J. Mech. Sci. 105976 (2020).

Porziani, S., Groth, C., Mancini, L., Cenni, R., Cova, M. & Biancolini, M.E. (2019): Optimisation of industrial parts by mesh morphing enabled automatic shape sculpting. Procedia Struct. Integrity 24, 724–737 (2019)

RBF Morph (2020), http://www.rbf-morph.com/act-module/. Accessed 29 July 2020

Stefano Porziani, Francesco de Crescenzo, Emanuele Lombardi, Christian Iandiorio, Pietro Salvini, Marco Evangelos Biancolini (2021): Automatic Optimization Method Based on Mesh Morphing Surface Sculpting Driven by Biological Growth Method: An Application to the Coiled Spring Section Shape, ICCS 2021, LNCS 12746, pp. 479–491, 2021

W. Kyle Anderson, V. Venkatakrishnan (1999): Aerodynamic design optimization on unstructured grids with a continuous adjoint formulation, Computers & Fluids 28 (1999) 443-480

ACKNOWLEDGEMENT

This research receives financial support from the Centre for Compressor Technology at City, University of London, Howden Compressors and Royal academy of engineering. The authors express their special gratitude to RBF Morph, Dr. Marco Evangelos Biancolini (Director of RBF Morph), Stefano Porziani & Marzia Di Battista for providing the student license and offering valuable feedback.